Journal of Neurochemistry

JOURNAL OF NEUROCHEMISTRY | 2010 | 113 | 1525–1535 doi: 10.1111/j.1471-4159.2010.06733.x

Restricted ketogenic diet enhances the therapeutic action of *N*-butyldeoxynojirimycin towards brain GM2 accumulation in adult Sandhoff disease mice

Christine A. Denny,*,[1] Karie A. Heinecke,* Youngho P. Kim,* Rena C. Baek,*,[2] Katrina S. Loh,*,[3] Terry D. Butters,† Roderick T. Bronson,‡ Frances M. Platt§ and Thomas N. Seyfried*

*Department of Biology, Boston College, Chestnut Hill, Massachusetts, USA

†The Glycobiology Institute, Department of Biochemistry, University of Oxford, South Parks Road, Oxford, UK

‡The Dana Farber/Harvard Comprehensive Cancer Center, Boston, Massachusetts, USA

§Department of Pharmacology, University of Oxford, Mansfield Road, Oxford, UK

Abstract

Sandhoff disease is an autosomal recessive, neurodegenerative disease involving the storage of brain ganglioside GM2 and asialo-GM2. Previous studies showed that caloric restriction, which augments longevity, and *N*-butyldeoxynojirimycin (*N*B-DNJ, Miglustat), an imino sugar that hinders the glucosyltransferase catalyzing the first step in glycosphingolipid biosynthesis, both increase longevity and improve motor behavior in the β-hexosaminidase (*Hexb*) knockout (–/–) murine model of Sandhoff disease. In this study, we used a restricted ketogenic diet (KD-R) and *N*B-DNJ to combat ganglioside accumulation. Adult *Hexb*–/– mice were placed into one of the following groups: (i) a standard diet (SD), (ii) a SD with *N*B-DNJ (SD + *N*B-DNJ), (iii) a KD-R, and (iv) a KD-R with *N*B-DNJ (KD-R + *N*B-DNJ). Forebrain GM2 content (μg sialic acid/100 mg dry wt) in the four groups was 375 ± 15, 312 ± 8, 340 ± 28, and 279 ± 26, respectively, indicating an additive interaction between *N*B-DNJ and the KD-R. Most interestingly, brain *N*B-DNJ content was 3.5-fold greater in the KD-R + *N*B-DNJ mice than in the SD + *N*B-DNJ mice. These data suggest that the KD-R and *N*B-DNJ may be a potential combinatorial therapy for Sandhoff disease by enhancing *N*B-DNJ delivery to the brain and may allow lower dosing to achieve the same degree of efficacy as high dose monotherapy.

Keywords: GA2, ganglioside, GM2, ketogenic diet, lysosomal storage disease, Sandhoff disease.

J. Neurochem. (2010) **113**, 1525–1535.

Sandhoff disease is an autosomal recessive GM2 gangliosidosis that results primarily in the storage of ganglioside GM2 and its asialo derivative GA2 as a result of a defect in the β-hexosaminidase (Hex) β-subunit gene. Sandhoff disease is characterized by the lack of the Hex A and B isoenzymes, while Tay-Sachs disease, another GM2 gangliosidosis, is characterized solely by the lack of Hex A. Both GM2 gangliosidoses are defined as having the failure to catabolyze GM2 to GM3 (Sandhoff and Kolter 2003). GM2 storage occurs primarily in neuronal lysosomes and leads to progressive neurodegeneration and brain dysfunction (Gravel *et al.* 1995). Furthermore, Sandhoff disease causes significant changes not only in neural tissues, but also in non-neural tissues, such as oligosaccharidiuria and hepatosplenomegaly (Tifft and Proia 2000).

The mouse model of Sandhoff disease was generated through the targeted disruption of the murine *Hexb* gene and

Received January 8, 2010; revised manuscript received March 10, 2010; accepted March 15, 2010.

Address correspondence and reprint requests to Thomas N. Seyfried, PhD, Boston College, Biology Department, Chestnut Hill, MA 02467, USA. E-mail: thomas.seyfried@bc.edu

[1]Present address: Department of Biological Sciences, Columbia University, New York, New York, USA

[2]Present address: Signal Transduction Program, The Burnham Institute for Medical Research, La Jolla, California, USA

[3]Present address: Division of Pulmonary, Allergy, and Critical Care Medicine, Columbia University College of Physicians and Surgeons, New York, New York, USA

Abbreviations used: β-OHB, β-hydroxybutyrate; BBB, blood-brain barrier; CR, caloric restriction; GD, Gaucher disease; GSL, glycosphingolipid; H&E, hematoxylin & eosin; Hex, β-hexosaminidase; HPTLC, high-performance TLC; KD, ketogenic diet; KD-R, restricted KD; LFB, luxol fast blue; LSDs, lysosomal storage diseases; *N*B-DNJ, *N*-butyldeoxynojirimycin; SD, standard diet; SRT, substrate reduction therapy.

is deficient in Hex A and B isoenzymes (Sango *et al.* 1995). *Hexb*−/− mice contain only about 1% of the wild-type hexosaminidase level, because of the presence of β-hexosaminidase S(αα). *Hexb*−/− mice are phenotypically indistinguishable from wild-type mice until adult ages (approximately 12 weeks of age) (Sango *et al.* 1995). Soon after, they rapidly begin to develop gait abnormalities and spastic hind limb movements, succumbing to death by 4–4.5 months of age. The *Hexb*−/− mice have been used to evaluate therapies for reducing glycosphingolipid (GSL) storage such as: bone marrow transplantation, enzyme replacement therapy, substrate reduction therapy, stem cell therapy, and caloric restriction (Norflus *et al.* 1998; Jeyakumar *et al.* 1999; Kasperzyk *et al.* 2004; Arfi *et al.* 2005; Baek *et al.* 2005; Denny *et al.* 2006).

N-butyldeoxynojirimycin (*N*B-DNJ/Zavesca™/Miglustat) is a reversible inhibitor of glucosylceramide synthase (GlcCerS), the enzyme that catalyzes the first step in the GSL biosynthetic pathway (Platt *et al.* 2003). In cellular and animal models of GSL storage disorders, *N*B-DNJ was efficacious in inhibiting ganglioside biosynthesis and in decreasing GSL storage (Platt *et al.* 1997; Jeyakumar *et al.* 1999). *N*B-DNJ has been approved for treatment of type 1 Gaucher disease (GD) world-wide (Cox *et al.* 2000; Elstein *et al.* 2004), and has recently been approved by the European Medicines Agency (EMEA) for Niemann-Pick type C disease. Previous reports showed that *N*B-DNJ is capable of penetrating the blood-brain barrier (BBB) (Treiber *et al.* 2007); however, the mechanism of *N*B-DNJ transport across the BBB has still not been elucidated (Begley *et al.* 2008).

Caloric restriction (CR), the reduction of nutrient intake without malnutrition, is a natural therapy that improves health and extends longevity (Weindruch and Walford 1988; Greene *et al.* 2001; Duan *et al.* 2003; Denny *et al.* 2006). CR has neuroprotective effects in rodent models of neurodegenerative diseases and has been shown to slow the progression of many age-related diseases, including brain cancer (Mukherjee *et al.* 2002). CR diminishes neuroinflammation and oxidative stress by decreasing the production of reactive oxygen species and glial activation (Morgan *et al.* 1999; Lee *et al.* 2000). The neuroprotective effects likely result from reduced glucose levels and elevated ketone bodies [β-hydroxybutyrate (β-OHB)], which increase energy efficiency (Greene *et al.* 2001; Mantis *et al.* 2003; Veech 2004; Mahoney *et al.* 2006). An example of a type of CR is the restricted ketogenic diet (KD-R), a high-fat, low carbohydrate diet that has been shown to have antiepileptic, anticonvulsant, and other neuroprotective effects (Mantis *et al.* 2003). We have previously shown that CR improves motor behavior and increases longevity in Sandhoff disease mice (Denny *et al.* 2006).

Here, we report that adult *Hexb*−/− mice treated with *N*B-DNJ had significantly less total forebrain ganglioside and GM2 content than non-*N*B-DNJ treated mice. *Hexb*−/− mice given a KD-R and *N*B-DNJ treatment had a 3.5-fold higher level of *N*B-DNJ detected in brain tissue than *Hexb*−/− mice given a standard diet (SD) + *N*B-DNJ treatment. These data suggest that the KD-R and *N*B-DNJ may be a potential combinatorial therapy for Sandhoff disease patients by allowing for increased absorption of *N*B-DNJ across the BBB into the primary diseased tissue.

Materials and methods

Mice

Mice heterozygous for the *Hexb* gene (Hexb +/–) were obtained as a gift from Dr. Richard Proia (National Institutes of Health, Bethesda, MD, USA) and were used to produce the homozygous knockout (−/−) mice. The mice were derived by homologous recombination and embryonic stem cell technology (Sango *et al.* 1995). Genotypes were determined by measuring hexosaminidase-specific activity in tail tissue according to the Galjaard procedure (Galjaard 1980; Hauser *et al.* 2004). All mice were propagated in the Boston College Animal Care Facility and were housed individually in plastic cages with filter tops containing Sani-Chip bedding (P.J. Murphy Forest Products Corp., Montville, NJ, USA). The room was maintained at 22°C on a 12-h light/12-h dark cycle. All animals were provided with cotton nesting pads for the duration of the experiment. All animal experiments were carried out with ethical committee approval in accordance with the National Institutes of Health Guide for the care and use of laboratory animals and were approved by the Institutional Animal Care and Use Committees of Boston College.

Dietary treatment

All mice received a standard diet of Prolab RMH 3000 chow (LabDiet, Richmond, IN, USA) prior to the experiment. The standard diet contains a balance of mouse nutritional ingredients and delivers 4.4 kcal/g gross energy, where fat, carbohydrate, protein, and fiber comprised 55, 520, 225, and 45 g/kg of the diet, respectively. After a 10-day pre-trial period, the mice were placed into four groups (n = 4–6 mice/group) in which the average body weight of each *Hexb*–/– group was similar. At 40 days of age, the mice were assigned to the following groups: (i) standard diet *ad libitum* (SD), (ii) SD *ad libitum* with *N*B-DNJ (SD + *N*B-DNJ), (iii) KD-R, and (iv) KD-R with *N*B-DNJ (KD-R + *N*B-DNJ).

The mice in the SD group received 80 *g* of food in the hopper every 2 days between 12 PM and 2 PM as in the pre-trial period until reaching 115 days of age. Daily food intake was estimated as the difference in food weight after 2 days divided in half. The mice in the KD-R groups received a KD that was obtained from Zeigler Bros., Inc. (Gardners, PA, USA) in butter-like form and contained a balance of mouse nutritional ingredients. The KD was matched to the SD for vitamins, minerals, and anti-oxidants (Todorova *et al.* 2000). According to the manufacturer's specification, the KD delivers 7.8 kcal/g gross energy, where fat, carbohydrate, protein, and fiber comprised 700, 0, 128, and 109 g/kg of the diet, respectively. The fat in this diet was derived from lard and the diet had a ketogenic ratio (fats: proteins + carbohydrates) of 5.48 : 1. After the 10-day pre-trial period, each mouse in the KD-R group was fasted 14 h before starting the KD.

Each mouse in the KD-R group served as its own control for body weight reduction. Based on food intake and body weight during the pre-trial period, food in the KD-R group was gradually reduced until each mouse achieved the target weight reduction of 15–18%. Body weight was used as an independent variable to reduce the variability among individual mice for the effects of CR (Pugh *et al.* 1999; Greene *et al.* 2001; Denny *et al.* 2006). The target body weight reduction for all KD-R *Hexb*–/– mice was reached in approximately 8–12 days. Food intake was measured daily and body weight was measured every 2 days. Food intake was either increased or decreased by an interval of approximately 0.2 g depending if the body weight was above or below the target weight reduction.

N-butyldeoxynojirimycin treatment

N-butyldeoxynojirimycin (*N*B-DNJ; 219.3 MW) was obtained as a gift from Oxford Glycosciences (Abingdon, UK). The *Hexb*–/– mice in the SD + *N*B-DNJ and the KD-R + *N*B-DNJ groups received diet mixed with 400 mg of *N*B-DNJ/kg body weight/day. The amount of *N*B-DNJ was calculated daily and mixed either with powdered SD or with KD-R. The KD-R and *N*B-DNJ was administered via a Petri dish attached to the side of the cage via a Velcro tab. The SD was grounded into a fine powder and mixed with the *N*B-DNJ; this mixture was administered in a small vial that was attached to the bottom of the cage via a Velcro tab to minimize possible food lost in the bedding. Unlike most glass feeding jars, which have a large mouth rim, vials were used with a small opening that did not permit nesting or digging through the SD. Since mice were individually housed, measurements of a pelleted food intake, powdered food intake, and powdered food intake with *N*B-DNJ were obtained. Food intake remained relatively constant when mice were switched from the pelleted form to powdered chow, and therefore, we are confident in our food and *N*B-DNJ administration.

N-butyldeoxynojirimycin was administered at 400 mg/kg/day to avoid a harsh body weight reduction in the KD-R + *N*B-DNJ mice. Previous studies showed that 600 mg/kg/day and 1200 mg/kg/day of *N*B-DNJ caused significant reduction in brain ganglioside content (Ranes *et al.* 2001). Since a KD-R was used in conjunction with *N*B-DNJ, we surmised that 600 or 1200 mg of *N*B-DNJ/kg/day would be too harsh on the *Hexb*–/– mice. A 400 mg of *N*B-DNJ/kg/day regimen was considered to be less stressful while achieving a similar reduction in total brain ganglioside content. The drug doses were most likely less than or equal to the desired 400 mg/kg/day since *N*B-DNJ was administered in the diet and a minimal amount could have been lost on the floor of the cage.

Measurement of plasma glucose and β-hydroxybutyrate

Blood was collected from mice on day 50 (the day before diet initiation), 75, and 115 (termination of experiment). The mice were anesthetized with isoflurane, USP (Halocarbon, River Edge, NJ, USA), and blood was collected from the retro-orbital sinus into heparinized tubes. The blood was centrifuged at 6000 *g* for 10 min, and the plasma was collected and stored at −80°C until assayed. Plasma glucose concentrations were measured spectrophotometrically using the StanBio® Enzymatic Glucose Assay (1075-102) (Stanbio Laboratory, Boerne, TX, USA). β-OHB concentrations were measured spectrophotometrically using a modification of the Williamson *et al.* (1962) enzymatic procedure.

Tissue processing

After killing by cervical dislocation at 115 days of age, brains were collected for lipid isolation, *N*B-DNJ content, and histologic analysis. The right hemisphere was sectioned into three pieces, weighed, and stored at −80°C. The left hemisphere was stored in Bouin's solution (LabChem Inc., Pittsburgh, PA, USA) at 4°C for histologic analysis.

Lipid isolation, purification, and quantification

Total lipids were isolated and purified from lyophilized forebrain tissue by using modifications of previously described procedures (Seyfried *et al.* 1978; Hauser *et al.* 2004; Kasperzyk *et al.* 2004; Denny *et al.* 2006). Neutral and acidic lipids were separated by using DEAE-Sephadex (A-25; Pharmacia Biotech, Upsala, Sweden) column chromatography as previously described (Macala *et al.* 1983; Seyfried *et al.* 1984; Kasperzyk *et al.* 2005; Denny *et al.* 2006). The total lipid extract, suspended in solvent A ($CHCl_3$: CH_3OH : H_2O, 30 : 60 : 8 by vol), was then applied to a DEAE-Sephadex column (1.2 mL bed volume) that had been equilibrated with solvent A. The column was washed twice with 20 mL of solvent A, and the entire neutral lipid fraction, consisting of the initial eluent plus washes, was collected. This fraction contained cholesterol, phosphatidylcholine, phosphatidylethanolamine, plasmologens, ceramide, sphingomyelin, cerebrosides, and asialo-GM2 (GA2). The acidic lipids were then eluted from the column with 30 mL solvent B ($CHCl_3$: CH_3OH : 0.8 M Na acetate, 30 : 60 : 8 by vol). This fraction contained the gangliosides and other less hydrophilic acidic lipids to include free fatty acids, cardiolipin, phosphatidylserine, phosphatidylinositol, phosphatidic acid, and sulfatides. The gangliosides were isolated and purified from other acidic lipids and analyzed by using the resorcinol assay as we previously described (Kasperzyk *et al.* 2005; Denny *et al.* 2006).

High-performance TLC

All lipids were analyzed qualitatively by high-performance TLC (HPTLC) according to previously described methods (Ando *et al.* 1978; Seyfried *et al.* 1978; Macala *et al.* 1983; Kasperzyk *et al.* 2005). Lipids were spotted on 10 × 20-cm Silica gel 60 HPTLC plates (E. Merck, Darmstadt, Germany) using a Camag Linomat III auto-TLC spotter (Camag Scientific Inc., Wilmington, NC, USA). To enhance precision, an internal standard (oleoyl alcohol) was added to the neutral and acidic lipid standards and samples as previously described (Macala *et al.* 1983; Kasperzyk *et al.* 2005). Purified lipid standards were purchased from Matreya Inc. (Pleasant Gap, PA, USA) or Sigma (St. Louis, MO, USA) or were a gift from Dr. Robert Yu (Medical College of Georgia, Augusta, GA, USA). The HPTLC plates were sprayed with either the resorcinol-HCl reagent or the orcinol-H_2SO_4 reagent and heated at 95°C for 30 min to visualize gangliosides or GA2, respectively (Kasperzyk *et al.* 2005; Denny *et al.* 2006). For neutral or acidic phospholipids, the plates were developed to a height of either 4.5 cm or 6 cm, respectively, with chloroform:methanol : acetic acid : formic acid : water (35 : 15 : 6 : 2 : 1 by vol), then developed to the top with hexanes:diisopropyl ether : acetic acid (65 : 35 : 2 by vol) as previously described (Macala *et al.* 1983; Seyfried *et al.* 1984). Neutral and acidic lipids were visualized by charring with 3% cupric acetate in 8% phosphoric acid solution, followed by heating in an oven at 160–170°C for 7 min.

The percentage distribution of the individual lipid bands was determined by scanning the plates on a Personal Densitometer SI with ImageQuant software (Molecular Dynamics, Sunnyvale, CA, USA) for gangliosides, acidic lipids, and neutral lipids or on a ScanMaker 4800 with ScanWizard5 V7.00 software (Microtek, Carson, CA, USA) for GA2.

N-butyldeoxynojirimycin extraction

N-butyldeoxynojirimycin was extracted and purified from mouse brain tissue (n = 3–4 mice/group) as previously described (Alonzi *et al.* 2008). Briefly, tissue samples were homogenized using an Ultra-Turrax T25 (Janke & Kunkel, IKA Labortechnik, Staufen, Germany) probe in 10% CH_3OH in dH_2O (v/v) at concentrations of 20–60 mg (wet weight)/mL. After addition of the imino sugar internal standard (*N*-propyl-DNJ), the homogenates were centrifuged at 100 000 *g* for 15 min at 2°C.

N-butyldeoxynojirimycin purification

N-butyldeoxynojirimycin was purified from mouse brain tissue as previously described (Mellor *et al.* 2000; Alonzi *et al.* 2008). Briefly, samples (400 μL) were centrifuged in a Millipore Ultrafree filter (Millipore, Bedford, MA, USA) at 4300 *g* for 60 min at 21°C and the filtrate was removed. dH_2O (300 μL) was added to the filter and centrifugation repeated. After a further wash with 300 μL water, all the three filtrates (900–1000 μL) were combined and adjusted to 50 mM with 1 M HCl. The filtrate was added to a pre-conditioned SCX column (Varian Bond Elut, Varian Inc., Palo Alto, CA, USA; 1 cc/100 mg) and eluted to waste. The column was washed with 1.5 mL of dH_2O and eluted to waste. Compound was eluted with 1% (v/v) NH_4 in CH_3OH and dried under vacuum. The compound was redissolved in dH_2O (500 μL) and added to a pre-conditioned C18 column (Waters Sep-Pak, Waters, Milford, MA, USA; 1 cc/100 mg) and washed with 2.5 mL dH_2O. Compound was eluted with CH_3OH, dried under vacuum, and redissolved in dH_2O for cation-exchange chromatographic analysis.

HPLC

Compounds purified were chromatographed in duplicate. The procedure of Mellor *et al.* (2000) was used for the separation, detection, and quantification of *N*-butyl-DNJ. The area under each peak corresponding to the internal standard and *N*-butyl-DNJ was measured and after application of a pre-determined response factor for the two compounds (Willenbrock *et al.* 1991), the amount of *N*B-DNJ was estimated.

Histology

The Bouin's-fixed left hemispheres were embedded in paraffin, sectioned at 5 μm, and stained with hematoxylin & eosin (H&E) and Luxol fast blue (LFB) at the Harvard University Rodent Histopathology Core Facility (Boston, MA, USA). Slides were examined by using a Zeiss AxioObserver A1 (Carl Zeiss MicroImaging, Inc., Thornwood, NY, USA) and an Axiocam Mrc CCD camera (Carl Zeiss MicroImaging Inc.).

Statistical analysis

Both analysis of variance (ANOVA) and a two-tailed *t*-test were used to evaluate the significance of differences between the SD, SD + *N*B-DNJ, KD-R, and KD-R + *N*B-DNJ groups. In each analysis, 3–6 independent mice were analyzed. Differences were considered significant at $p < 0.05$. All values are expressed as mean ± SEM.

Results

Influence of diet and *N*B-DNJ on body weight

All mice were housed individually from the start of the pre-trial period, and were matched for age (40 days of age) and body weight at the beginning of the dietary treatment (Fig. 1a). At 50 days of age, the two KD-R groups were fasted for approximately 14 h before starting the respective diets. Body weights of the KD-R groups dropped at 50 days of age because of the restriction of caloric intake to reach a 15–18% body weight reduction in each mouse. The body weights were stabilized in the KD-R groups for the next 20 days. *N*B-DNJ was added to the diet of the respective groups at 85 days of age. Whereas the body weights remained unchanged in the KD-R + *N*B-DNJ mice, the body weights declined in the SD + *N*B-DNJ mice following *N*B-DNJ administration. The body weight reduction following *N*B-DNJ treatment was consistent with previous observations for this drug (Priestman *et al.* 2008). After the initial body weight decline from *N*B-DNJ administration, body weights increased gradually in the KD-R + *N*B-DNJ group, ultimately achieving weights similar to those of the KD-R mice at the time of killing.

Influence of diet and *N*B-DNJ on food intake

The KD-R diet was initiated at 50 days of age (Fig. 1b). After an initial 15–18% body weight reduction, food administration was gradually increased in the KD-R mouse groups for them to parallel the age-related body weight increase of the SD mouse groups. The food intake of the SD groups remained similar until 85 days of age when *N*B-DNJ treatment was initiated. Food administration was slightly increased in the *N*B-DNJ groups to offset the initial drug-induced decline in body weight. When *N*B-DNJ was added to the SD diet, the mice increased food intake over that of the SD control group, but still lost body weight (Fig. 1a and b).

Influence of diet and *N*B-DNJ on plasma glucose and β-hydroxybutyrate

The plasma glucose and β-OHB levels were measured at different time points of the study (Fig. 1c and d). Plasma glucose and β-OHB levels of all mice were approximately 13 mM and 0.5 mM, respectively, prior to diet therapy and drug initiation. At 75 days of age (25 days into the diet therapy), plasma glucose levels of the KD-R groups were significantly less than those of the SD groups ($p < 0.01$), and the β-OHB levels of the KD-R groups were significantly greater than those of the SD groups ($p < 0.01$). Plasma glucose levels were similar in the KD-R and SD groups at the time of the study termination (115 days of age). The plasma

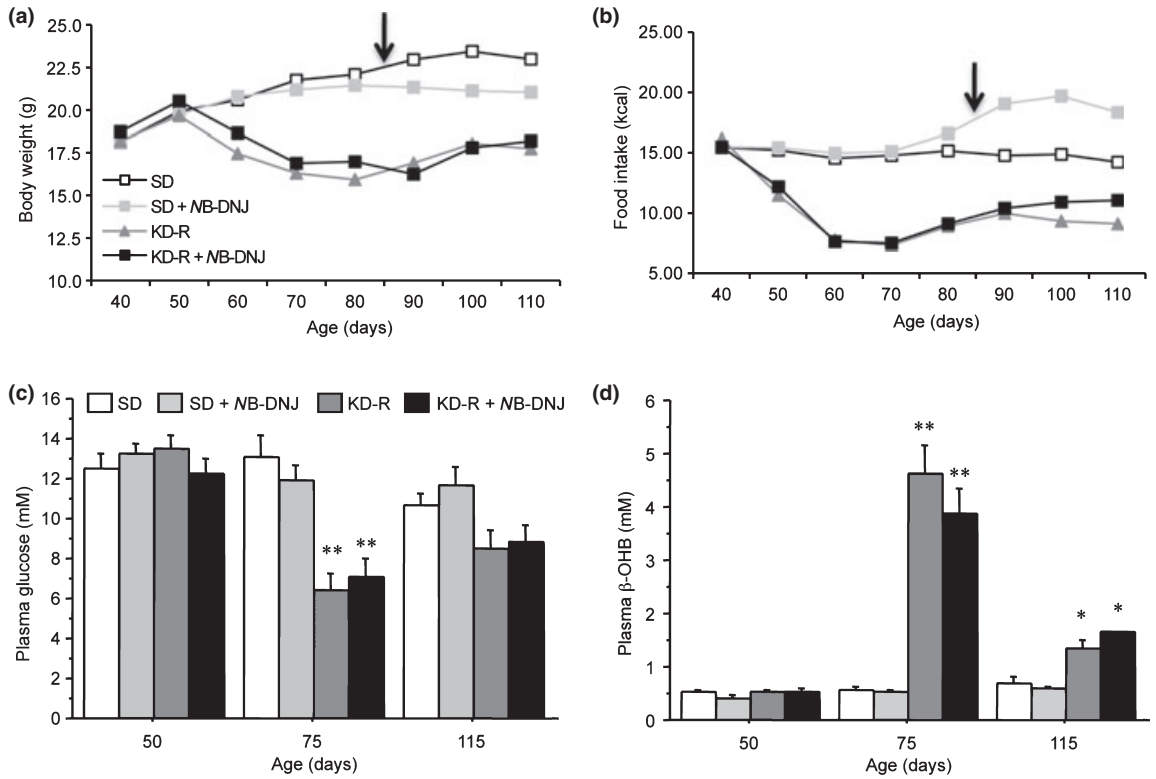

Fig. 1 Influence of ketogenic diet (KD) and *N*-butyldeoxynojirimycin (*N*B-DNJ) on body weight (a), food intake (b), plasma glucose (c), and plasma β-hydroxybutyrate (β-OHB) (d) levels in adult *Hexb*–/– mice. Mice were separated into individual cages at 40 days of age and dietary groups were initiated at 50 days of age. Drug treatment was initiated at day 85 as indicated by arrows. Plasma β-OHB and glucose levels were similar in all groups of mice at 50 days of age. At 75 days of age, glucose levels were significantly lower and β-OHB levels were significantly higher in the restricted KD (KD-R) groups when compared with the standard diet (SD) groups. At 115 day of age, plasma glucose levels were only significantly different between the KD-R and SD + *N*B-DNJ mice. Plasma β-OHB levels of the KD-R and the KD-R + *N*B-DNJ mice were significantly higher than those of the SD mice. $n = 4–6$ mice/group. Error bars represent ± SEM. $^{*}p < 0.05$, $^{**}p < 0.01$.

glucose levels of the KD-R mice (8.5 ± 0.9 mM) were significantly less than those of SD + *N*B-DNJ mice (11.7 ± 0.9 mM), reflecting the significantly different food intake between the groups ($p < 0.05$). Furthermore, the plasma β-OHB levels of the KD-R and the KD-R + *N*B-DNJ mice were significantly greater than those of the SD mice ($p < 0.05$).

Influence of diet and *N*B-DNJ on forebrain lipids

To determine if the KD-R and/or *N*B-DNJ-induced changes in plasma glucose and β-hydroxybutyrate were associated with an alteration in the primary phenotype of ganglioside accumulation, we assessed forebrain ganglioside content and distribution in the treated *Hexb*–/– mice. Consistent with our previous findings using CR alone (Denny *et al.* 2006), the KD-R caused no significant changes in total forebrain ganglioside concentration, as measured by ganglioside sialic acid (μg/100 mg dry weight), in the *Hexb*–/– mice (Table 1). However, total forebrain ganglioside content was significantly lower in the *N*B-DNJ treated mice than in the non-*N*B-DNJ treated mice. It is important to note that the dose of *N*B-DNJ administered is much lower than published studies and therefore, the reduction in total forebrain ganglioside content is less than usually published. In addition, the KD-R and/or *N*B-DNJ had no significant effect on forebrain water content, a general marker for brain maturation (Seyfried *et al.* 1978), or asialo-GM2 (GA2) content (Table 1 and Fig. 2b).

The influence of KD-R and/or *N*B-DNJ on the qualitative and quantitative distribution of individual gangliosides in the *Hexb*–/– mice is shown in Table 2 and Fig. 2a. GM2 was the major ganglioside in the *Hexb*–/– mice. GM2 is mostly undetectable in the brains of heterozygous or wild-type mice at these ages (Denny *et al.* 2006). While the KD-R did not significantly reduce GM2 levels, *N*B-DNJ significantly reduced GM2 levels in both groups of treated mice. Interestingly, GD1b content was significantly lower in the KD-R + *N*B-DNJ mice when compared with both SD groups. No significant changes were found among the groups for the distribution of other gangliosides.

The influence of KD-R and/or *N*B-DNJ on the qualitative and quantitative distribution of neutral and acidic forebrain

Table 1 Glycosphingolipid content in *Hexb*−/− mice[a]

Strain	*n*[b]	Water content (%)	Ganglioside sialic acid (μg/100 mg dry weight)	GA2[c] (mg/100 mg dry weight)	*N*B-DNJ Concentration nmol/g tissue
SD	6	76.5 ± 0.1	875 ± 24	4.1 ± 0.05	–
SD + *N*B-DNJ	5	76.2 ± 0.6	795 ± 18*	3.9 ± 0.13	0.33 ± 0.15
KD-R	4	75.1 ± 1.1	821 ± 27	4.0 ± 0.18	–
KD-R + *N*B-DNJ	4	77.7 ± 0.7	743 ± 34*	4.0 ± 0.04	1.16 ± 0.04**

[a]Values represent the mean ± SEM.
[b]*n*, the number of independent mice analyzed.
[c]Determined from densitometric scanning of high-performance TLC as shown in Fig 2b.
*Indicates that the value is significantly different from that of the SD mice at $p < 0.05$ as determined from the two-tailed *t*-test.
**Indicates that the value is significantly different from that of the SD + *N*B-DNJ mice at $p < 0.01$ as determined from the two-tailed *t*-test.
SD, standard diet; *N*B-DNJ, *N*-butyldeoxynojirimycin; KD-R, restricted ketogenic diet.

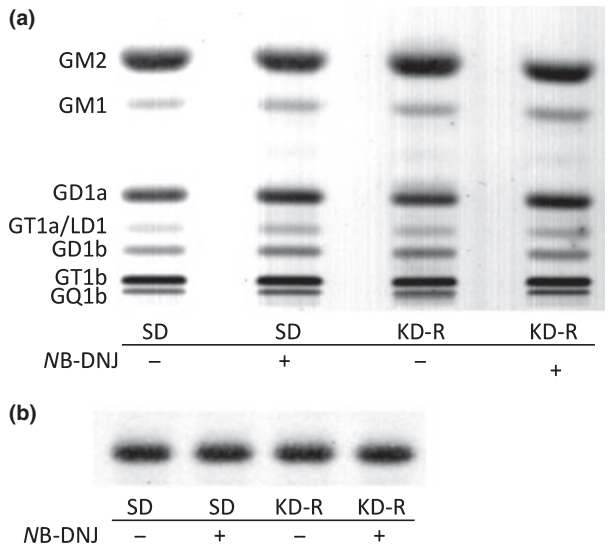

Fig. 2 High-performance TLC of forebrain gangliosides (a) and asialo-GM2 (b) in adult *Hexb*−/− mice. The amount of ganglioside sialic acid spotted per lane was equivalent to approximately 1.5 μg, and the amount of lipid spotted per lane was equivalent to approximately 200 μg dry weight. For gangliosides and asialo-GM2, the plate was developed by a single ascending run with $CHCl_3$: CH_3OH : dH_2O (55 : 45 : 10 by vol) containing 0.02% $CaCl_2$ $2H_2O$ or with $CHCl_3$: CH_3OH : dH_2O (65 : 35 : 8 by vol), respectively. The bands were visualized with resorcinol-HCl spray for gangliosides, or with orcinol-H_2SO_4 spray for asialo-GM2.

lipids in the *Hexb*−/− mice is shown in Table 3 and Fig. 3a and b. No significant differences were observed in the distribution of neutral or acidic lipids, to include phospholipids.

Influence of diet and *N*B-DNJ on *N*B-DNJ concentration in cortex

N-butyldeoxynojirimycin concentrations were measured in the brain of both *N*B-DNJ-treated groups. Surprisingly, the content of *N*B-DNJ was 3.5-fold higher in the cortex of KD-R + *N*B-DNJ mice than in the cortex of SD + *N*B-DNJ mice (Table 1). These findings indicate that the KD-R significantly facilitates *N*B-DNJ uptake into brain tissue.

Influence of diet and *N*B-DNJ on brain morphology

Sagittal sections of the left hemisphere were stained with LFB and H&E to visualize storage material and morphology (Fig. 4). The cytoplasm of neurons was enlarged and contained pale-staining inclusion material in lysosomes in sections of the cortex stained with H&E (Fig. 4a). In sections stained with LFB, myelin tracts in the cerebellum appeared similar in all *Hexb*−/− mice (Fig. 4b). Furthermore, all groups had Purkinje cells in which the cytoplasm in these cells appeared punctate as a result of the swelling of multiple lysosomes. (Fig. 4c). These findings indicate that the combined treatments did not noticeably reduce histologic storage material in the *Hexb*−/− mice.

Discussion

We found an additive interaction of a KD-R and substrate reduction therapy (SRT) using *N*B-DNJ in adult Sandhoff disease mice. No previous studies have evaluated the effects of dietary treatment and SRT in combination on disease progression in any of the lysosomal storage diseases (LSDs). Total forebrain ganglioside content and GM2 content were significantly reduced in both *N*B-DNJ treated groups when compared with non-*N*B-DNJ treated groups. Surprisingly, the content of *N*B-DNJ in brain tissue was significantly greater in the KD-R + *N*B-DNJ mice than in the SD + *N*B-DNJ mice, suggesting that the combinatorial diet and drug therapy is superior in facilitating *N*B-DNJ absorption into the brain and may allow lower dosing of *N*B-DNJ to achieve the same degree of efficacy as high dose monotherapy.

Weight loss is a common side effect experienced by patients taking *N*B-DNJ for type I Gaucher disease (Cox *et al.* 2000; Elstein *et al.* 2004; Giraldo *et al.* 2006). In the

Table 2 Forebrain ganglioside distribution in *Hexb*–/– mice[a]

		Concentration (μg/100 mg dry weight)[c]						
	n[b]	GM2	GM1	GD1a	GT1a/LD1	GD1b	GT1b	GQ1b
SD	6	375 ± 15	51 ± 7	161 ± 12	19 ± 2	53 ± 3	151 ± 8	58 ± 14
SD + *N*B-DNJ	5	312 ± 8**	46 ± 3	157 ± 10	19 ± 2	52 ± 3	144 ± 9	66 ± 5
KD-R	4	340 ± 28	50 ± 8	155 ± 15	18 ± 3	50 ± 3	147 ± 10	61 ± 12
KD-R + *N*B-DNJ	4	272 ± 26**	40 ± 5	176 ± 14	18 ± 1	41 ± 3*	138 ± 6	58 ± 9

[a]Values represent the mean ± SEM.
[b]n, the number of independent mice analyzed.
[c]Determined from densitometric scanning of high-performance TLC as shown in Fig 2.
*Indicates that the value is significantly different from that of the SD mice at $p < 0.05$ as determined from the two-tailed t-test.
**Indicates that the value is significantly different from that of the SD mice at $p < 0.01$ as determined from the two-tailed t-test.
SD, standard diet; *N*B-DNJ, *N*-butyldeoxynojirimycin; KD-R, restricted ketogenic diet.

Table 3 Forebrain neutral and acidic lipid distribution in *Hexb*–/– mice[a]

		Concentration (mg/100 mg dry weight)[c]			
		Neutral		Acidic	
Groups	n[b]	Cerebrosides	Phosphatidylcholine	Sulfatides	Phosphatidylinositol
SD	6	2.0 ± 0.2	4.2 ± 0.4	0.46 ± 0.07	0.54 ± 0.04
SD + *N*B-DNJ	5	1.9 ± 0.2	3.3 ± 0.3	0.44 ± 0.02	0.51 ± 0.01
KD	5	1.8 ± 0.1	3.7 ± 0.3	0.45 ± 0.01	0.47 ± 0.05
KD + *N*B-DNJ	4	1.8 ± 0.5	4.2 ± 0.3	0.43 ± 0.11	0.57 ± 0.08

[a]Values represent the mean ± SEM.
[b]n, the number of independent mice analyzed.
[c]Determined from densitometric scanning of high-performance TLC as shown in Fig 3.
SD, standard diet; *N*B-DNJ, *N*-butyldeoxynojirimycin; KD, ketogenic diet.

first clinical trial with *N*B-DNJ, Cox *et al.* (2000) reported diarrhea as being the most frequent adverse effect in 79% of the patients. We found that the mice treated with KD-R + *N*B-DNJ maintained a constant body weight following the addition of *N*B-DNJ, whereas the SD + *N*B-DNJ mice lost body weight although their food consumption was the highest of all the groups. Priestman *et al.* (2008) reported that *N*B-DNJ caused weight loss as a result of appetite suppression in lean and obese mice. However, these studies were conducted with a *N*B-DNJ dose of 2400 mg/kg body weight/day in the diet, whereas our study used a dose of only 400 mg/kg body weight/day in the diet. The side effect of reduced food consumption previously reported was not associated with a lower dose of *N*B-DNJ as our data show. Our data also suggest that *N*B-DNJ administered with the KD-R might allow for a decreased dose to be administered and thereby achieve the same benefits by reducing side effects such as severe weight loss.

Alternatively, it is possible that the fat composition of the KD allowed for body weight stability. *N*B-DNJ inhibits the disaccharidases, sucrase, and maltase (Andersson *et al.* 2000) and the glycogen debranching enzymes (Andersson *et al.* 2004). Inhibition of the disaccharidases in the gastrointestinal tract may result in reduced post-prandial absorption of monosaccharides (Priestman *et al.* 2008), while inhibition of glycogen debranching enzymes results in inhibition in glycogenolysis, and therefore, the inability to breakdown glycogen. Therefore, a diet mainly composed of fat may allow for increased nutrient absorption that would otherwise be inhibited by *N*B-DNJ given with a diet mainly composed of carbohydrates. Using an alternate fuel source (i.e. fat) could not only allow patients to maintain a consistent body weight, but may also prevent the severe diarrhea that is often seen in LSD patients on *N*B-DNJ. Future studies will be necessary to determine if the KD-R is effective in preventing weight loss and diarrhea in patients with LSDs.

We previously showed that CR induced improvements in survival and motor behavior of Sandhoff disease mice without reducing GSL storage (Denny *et al.* 2006). Our new results with the KD-R are in accord with our previous data and show no obvious dietary-induced alterations in the forebrain lipid profile. Conversely, *N*B-DNJ has been shown

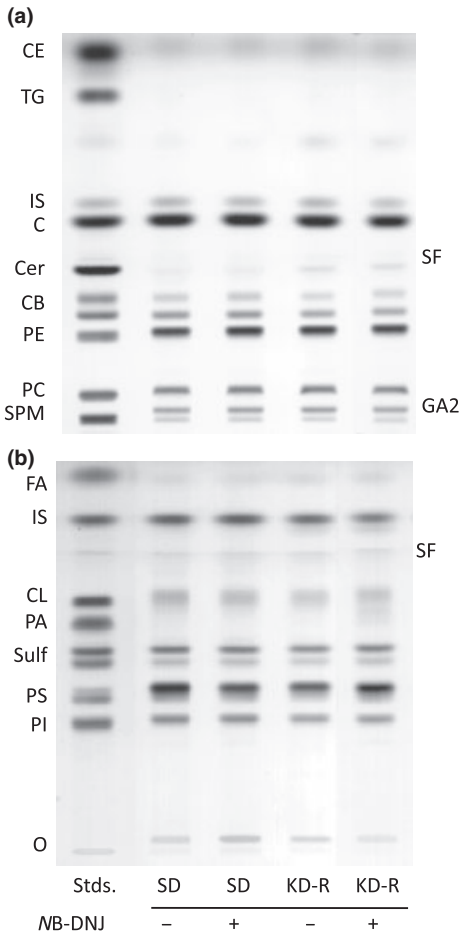

Fig. 3 High-performance TLC of forebrain neutral lipids (a) and acidic lipids (b) in adult *Hexb*–/– mice. The amount of neutral lipids and acidic lipids spotted per lane was equivalent to approximately 70 μg and 200 μg tissue dry weight, respectively. The plates were developed as described in Materials and methods. *Neutral Lipids*: CE, cholesterol esters; TG, triglycerides; C, cholesterol; CM, ceramide; CB, cerebrosides (doublet); PE, phosphatidylethanolamine; PC, phosphatidylcholine; GA2, asialo-GM2; SPM, sphingomyelin. *Acidic lipids*: FA, fatty acids; C, cholesterol; CL, cardiolipin; PA, phosphatidic acid; Sulf, sulfatides (doublet); PS, phosphatidylserine; PI, phosphatidylinositol. IS, internal standard; O, origin; and SF, solvent front of the first developing solvent system.

to improve survival and delay symptom onset by reducing GSL accumulation, to include GM2 (Jeyakumar *et al.* 1999, 2001). Our *N*B-DNJ data also support these studies: total forebrain ganglioside content and GM2 content were significantly reduced in both *N*B-DNJ treated groups when compared with non-*N*B-DNJ treated groups. All other lipids, with the exception of GD1b, were unaltered by *N*B-DNJ. Forebrain GD1b content was lower in the KD-R + *N*B-DNJ mice than in the mice receiving the SD. Interestingly, two previous reports have indicated that high levels of GD1b were associated with prominent cerebellar ataxia and that low GD1b levels may be related to a delayed occurrence of cerebellar ataxia (Sugimoto *et al.* 2002; Bae and Kim 2005). Further studies will be necessary to determine if the KD-R given with *N*B-DNJ improves additional motor behaviors through alterations in GD1b.

In addition to having elevated GM2 levels, *Hexb*–/– mice also store significant amounts of GA2. In accord with our previous studies (Kasperzyk *et al.* 2004; Baek *et al.* 2008), *N*B-DNJ reduced GM2 levels in adult SD mice, but GA2 levels remained unaltered. This is surprising since GA2 is derived from GM2 by sialidase. Baek *et al.* (2008), using a synthetic substrate 4-methylumbelliferone-neuraminic acid, showed a slight, but significant increase in brain sialidase activity in neonatal *N*-butyldeoxygalactonojirimycin-treated mice when compared with control mice, suggesting that the unaltered brain GA2 levels could result from increased sialidase activity. It is therefore possible that enhanced sialidase from either of the SRT treatments might mask a potential reduction in GA2. Future studies, in which GM2 is used as the substrate and not 4-methylumbelliferone-neuraminic acid, are planned to monitor sialidase activity towards GM2 throughout the treatments.

Storage material in the *Hexb*–/– mice is extensive in many neurons of the central nervous system, to include those in the CA3 region of hippocampus and in the Purkinje cells of the cerebellum (Sango *et al.* 1995). Consistent with our previous results using CR (Denny *et al.* 2006), we did not detect any major differences in morphology from either treatment using H&E or LFB staining. It is unlikely that major morphological differences would occur from either treatment for numerous reasons. Firstly, *N*B-DNJ was initiated in adulthood and therefore, extensive GSL storage had already occurred. This is consistent with previous studies showing that if *N*B-DNJ therapy was commenced at 11 weeks of age, there was no increase in life expectancy, suggesting that an irreversible disease process had already commenced (Jeyakumar *et al.* 1999). Secondly, although GM2 storage was significantly reduced by our *N*B-DNJ treatment, there was still a substantial amount of GM2 present in the forebrain. Conversely, GM2 is present in only trace amounts in wild-type mice (Denny *et al.* 2006). Taken together, these data suggest that storage morphology following either treatment is most likely unaltered because of the late age at which treatment was initiated. Future studies, in which *N*B-DNJ treatment would be started in the early pre-symptomatic period, could possibly clear storage and a more normal neuronal morphology might emerge.

Most interestingly, we found that the content of *N*B-DNJ in brain tissue was significantly (3.5-fold) greater in the KD-R + *N*B-DNJ mice than in the SD + *N*B-DNJ mice, suggesting that the KD-R might facilitate *N*B-DNJ uptake and transport across the BBB. *N*B-DNJ has an acyl side chain of 4 carbon atoms, is freely soluble in water, and is generally believed to cross the BBB to achieve substrate reduction (Platt *et al.* 1997; Norflus *et al.* 1998). However, if lipid

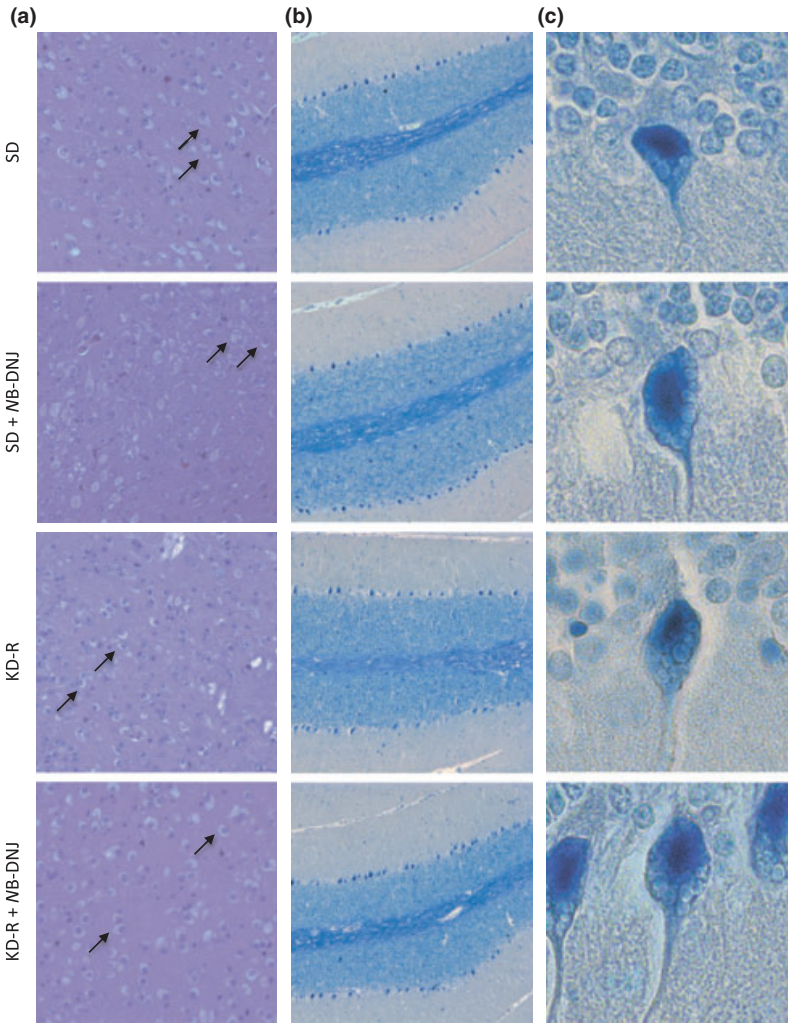

Fig. 4 Hematoxylin & eosin staining of cortex in *Hexb*–/– mice (a). Arrows indicate swollen neurons. Luxol fast blue staining of myelin (b) and of Purkinje cells (c) in the cerebellum of adult *Hexb*–/– mice. Images were taken at 40×. Sagittal sections taken at 5 μm.

solubility and total polar surface area were used to assess the potential of *N*B-DNJ for optimal BBB permeability, *N*B-DNJ would be considered marginal (Begley *et al.* 2008). On the other hand, ketone bodies (i.e. β-hydroxybutyrate) are actively transported across the BBB, particularly during fasting and caloric restriction (Gjedde and Crone 1975; Pollay and Stevens 1980; Hasselbalch *et al.* 1995). We suggest that the active transport of ketone bodies across the BBB might also increase the transport of *N*B-DNJ. The neuroprotective effects of the KD-R, such as reducing reactive oxygen species, could also account for the increased *N*B-DNJ uptake into the brain. The KD-R could allow for facilitated transport of *N*B-DNJ across the BBB by simply increasing ketone bodies directly and thereby, increasing ketone assisted absorption of *N*B-DNJ. The KD-R could also have an indirect effect on *N*B-DNJ transportation by altering transporters or endothelial cells of the BBB. Alternatively, the KD-R could enhance the uptake of *N*B-DNJ by mucosal cells in the intestines and thereby, result in higher concentrations reaching the circulation and being available for transport across the BBB. Future *in vitro* studies will be necessary to determine the mechanism by which the KD-R increases *N*B-DNJ transport in cells.

In summary, our results show that *N*B-DNJ is effective in decreasing total forebrain ganglioside content and GM2 content in a mouse model of Sandhoff disease. Furthermore, when *N*B-DNJ was administered with the KD-R, the content of *N*B-DNJ in brain tissue was 3.5-fold greater in the KD-R + *N*B-DNJ mice than in the SD + *N*B-DNJ mice. We contend that the most effective therapeutic strategy for the life-long management of Sandhoff disease and possibly other LSDs should involve combinatorial therapies, to include SRT (*N*B-DNJ, *N*-butyldeoxygalactonojirimycin), enzyme replacement therapy (neural stem cells), and anti-inflammatory approaches (CR and non-steroidal anti-inflammatory drugs). We now propose using the KD-R as a new facilitator for *N*B-DNJ absorption into the brain. Further evaluation of the proposed therapies will not only aid in understanding the

pathogenesis of Sandhoff disease, but will also aid in designing better therapeutics.

Acknowledgements

We thank John Mantis and Aurelien Bergmann for excellent technical assistance. This work was supported in part by NIH grant NS055195, Boston College Research Expense Fund, and the National Tay-Sachs and Allied Disease Association, Inc. (NTSAD).

References

Alonzi D. S., Neville D. C. A., Lachmann R. H., Dwek R. A. and Butters T. D. (2008) Glucosylated free oligosaccharides are biomarkers of endoplasmic-reticulum alpha-glucosidase inhibition. *Biochem. J.* **409**, 571–580.

Andersson U., Butters T. D., Dwek R. A. and Platt F. M. (2000) *N*-butyldeoxygalactonojirimycin: a more selective inhibitor of glycosphingolipid biosynthesis than *N*-butyldeoxynojirimycin, in vitro and in vivo. *Biochem. Pharmacol.* **59**, 821–829.

Andersson U., Reinkensmeier G., Butters T., Dwek R. A. and Platt F. M. (2004) Inhibition of glycogen breakdown by imino sugars in vitro and in vivo. *Biochem. Pharmacol.* **67**, 697–705.

Ando S., Chang N. C. and Yu R. K. (1978) High-performance thin-layer chromatography and densitometric determination of brain ganglioside compositions of several species. *Anal. Biochem.* **89**, 437–450.

Arfi A., Bourgoin C., Basso L. *et al.* (2005) Bicistronic lentiviral vector corrects beta-hexosaminidase deficiency in transduced and cross-corrected human Sandhoff fibroblasts. *Neurobiol. Dis.* **20**, 583–593.

Bae J. S. and Kim B. J. (2005) Cerebellar ataxia and acute motor axonal neuropathy associated with Anti GD1b and Anti GM1 antibodies. *J. Clin. Neurosci.* **12**, 808–810.

Baek R. C., Lee J. P., Seyfried T. N. and Snyder E. Y. (2005) Neural stem cell transplantation reduces brain GM2 and GA2 content in a mouse model of Sandhoff disease. *J. Neurochem.* **94**, 21.

Baek R. C., Kasperzyk J. L., Platt F. M. and Seyfried T. N. (2008) *N*-butyldeoxygalactonojirimycin reduces brain ganglioside and GM2 content in neonatal Sandhoff disease mice. *Neurochem. Int.* **52**, 1125–1133.

Begley D., Pontikis C. and Scarpa M. (2008) Lysosomal storage diseases and the blood-brain barrier. *Curr. Pharm. Des.* **14**, 1566–1580.

Cox T., Lachmann R., Hollak C. *et al.* (2000) Novel oral treatment of Gaucher's disease with *N*-butyldeoxynojirimycin (OGT 918) to decrease substrate biosynthesis. *Lancet* **355**, 1481–1485.

Denny C. A., Kasperzyk J. L., Gorham K. N., Bronson R. T. and Seyfried T. N. (2006) Influence of caloric restriction on motor behavior, longevity, and brain lipid composition in Sandhoff disease mice. *J. Neurosci. Res.* **83**, 1028–1038.

Duan W., Guo Z., Jiang H., Ware M., Li X. J. and Mattson M. P. (2003) Dietary restriction normalizes glucose metabolism and BDNF levels, slows disease progression, and increases survival in huntingtin mutant mice. *Proc. Natl Acad. Sci. USA* **100**, 2911–2916.

Elstein D., Hollak C., Aerts J. M. F. G. *et al.* (2004) Sustained therapeutic effects of oral miglustat (Zavesca, *N*-butyldeoxynojirimycin, OGT 918) in type I Gaucher disease. *J. Inherit. Metab. Dis.* **27**, 757–766.

Galjaard H. (1980) *Genetic Metabolic Disease: Diagnosis and Prenatal Analysis*. Elsevier Sicence Publishers, Amsterdam.

Giraldo P., Latre P., Alfonso P. *et al.* (2006) Short-term effect of miglustat in every day clinical use in treatment-naïve or previously treated patients with type 1 Gaucher's disease. *Haematologica* **91**, 703–706.

Gjedde A. and Crone C. (1975) Induction processes in blood-brain transfer of ketone bodies during starvation. *Am. J. Physiol.* **229**, 1165–1169.

Gravel R. A., Clarke J. T. R., Kaback M. M., Mahuran D., Sandhoff K. and Suzuki K. (1995) The GM2 gangliosidoses. in *The Metabolic and Molecular Bases of Inherited Disease* (Scriver C. R., Beaudet A. L., Sly W. S. and Valle D., eds), Vol. II, pp. 2839–2879. McGraw-Hill, Inc., New York.

Greene A. E., Todorova M. T., McGowan R. and Seyfried T. N. (2001) Caloric restriction inhibits seizure susceptibility in epileptic EL mice by reducing blood glucose. *Epilepsia* **42**, 1371–1378.

Hasselbalch S. G., Knudsen G. M., Jakobsen J., Hageman L. P., Holm S. and Paulson O. B. (1995) Blood-brain barrier permeability of glucose and ketone bodies during short-term starvation in humans. *Am. J. Physiol.* **268**, E1161–E1166.

Hauser E. C., Kasperzyk J. L., d'Azzo A. and Seyfried T. N. (2004) Inheritance of lysosomal acid b-galactosidase activity and gangliosides in crosses of DBA/2J and knockout mice. *Biochem. Genet.* **42**, 241–257.

Jeyakumar M., Butters T. D., Cortina-Borja M., Hunnam V., Proia R. L., Perry V. H., Dwek R. A. and Platt F. M. (1999) Delayed symptom onset and increased life expectancy in Sandhoff disease mice treated with *N*-butyldeoxynojirimycin. *Proc. Natl Acad. Sci. USA* **96**, 6388–6393.

Jeyakumar M., Norflus F., Tifft C. J., Cortina-Borja M., Butters T. D., Proia R. L., Perry V. H., Dwek R. A. and Platt F. M. (2001) Enhanced survival in Sandhoff disease mice receiving a combination of substrate deprivation therapy and bone marrow transplantation. *Blood* **97**, 327–329.

Kasperzyk J. L., El-Abbadi M. M., Hauser E. C., D'Azzo A., Platt F. M. and Seyfried T. N. (2004) *N*-butyldeoxygalactonojirimycin reduces neonatal brain ganglioside content in a mouse model of GM1 gangliosidosis. *J. Neurochem.* **89**, 645–653.

Kasperzyk J. L., d'Azzo A., Platt F. M., Alroy J. and Seyfried T. N. (2005) Substrate reduction therapy reduces ganglioside content in postnatal cerebrum-brainstem and cerebellum in a mouse model of GM1 gangliosidosis. *J. Lipid Res.* **46**, 744–751.

Lee C. K., Weindruch R. and Prolla T. A. (2000) Gene-expression profile of the ageing brain in mice. *Nat. Genet.* **25**, 294–297.

Macala L. J., Yu R. K. and Ando S. (1983) Analysis of brain lipids by high performance thin-layer chromatography and densitometry. *J. Lipid Res.* **24**, 1243–1250.

Mahoney L. B., Denny C. A. and Seyfried T. N. (2006) Caloric restriction in C57BL/6J mice mimics therapeutic fasting in humans. *Lipids Health Dis.* **5**, 13.

Mantis J. G., Centeno N., Todorova M. T., McGowan R. and Seyfried T. N. (2003) Metabolic control of epilepsy in adult EL mice with the ketogenic diet and caloric restriction. *Epilepsia* **44**(Suppl. 9), 64–65.

Mellor H. R., Adam A., Platt F. M., Dwek R. A. and Butters T. D. (2000) High-performance cation-exchange chromatography and pulsed amperometric detection for the separation, detection, and quantitation of N-alkylated imino sugars in biological samples. *Anal. Biochem.* **284**, 136–142.

Morgan T. E., Xie Z., Goldsmith S., Yoshida T., Lanzrein A.-S., Stone D., Rozovsky I., Perry G., Smith M. A. and Finch C. E. (1999) The mosaic of brain glial hyperactivity during normal ageing and its attenuation by food restriction. *Neuroscience* **89**, 687–699.

Mukherjee P., El-Abbadi M. M., Kasperzyk J. L., Ranes M. K. and Seyfried T. N. (2002) Dietary restriction reduces angiogenesis and

growth in an orthotopic mouse brain tumour model. *Br. J. Cancer* **86**, 1615–1621.

Norflus F., Tifft C. J., McDonald M. P., Goldstein G., Crawley J. N., Hoffmann A., Sandhoff K., Suzuki K. and Proia R. L. (1998) Bone marrow transplantation prolongs life span and ameliorates neurologic manifestations in Sandhoff disease mice. *J. Clin. Invest.* **101**, 1881–1888.

Platt F. M., Neises G. R., Reinkensmeier G., Townsend M. J., Perry V. H., Proia R. L., Winchester B., Dwek R. A. and Butters T. D. (1997) Prevention of lysosomal storage in Tay-Sachs mice treated with N- butyldeoxynojirimycin. *Science* **276**, 428–431.

Platt F. M., Jeyakumar M., Andersson U., Heare T., Dwek R. A. and Butters T. D. (2003) Substrate reduction therapy in mouse models of the glycosphingolipidoses. *Philos. Trans. R. Soc. Lond. B Biol. Sci.* **358**, 947–954.

Pollay M. and Stevens F. A. (1980) Starvation-induced changes in transport of ketone bodies across the blood-brain barrier. *J. Neurosci. Res.* **5**, 163–172.

Priestman D. A., van der Spoel A. C., Butters T. D., Dwek R. A. and Platt F. M. (2008) *N*-butyldeoxynojirimycin causes weight loss as a result of appetite suppression in lean and obese mice. *Diabetes Obes. Metab.* **10**, 159–166.

Pugh T. D., Klopp R. G. and Weindruch R. (1999) Controlling caloric consumption: protocols for rodents and rhesus monkeys. *Neurobiol. Aging* **20**, 157–165.

Ranes M. K., El-Abbadi M., Manfredi M. G., Mukherjee P., Platt F. M. and Seyfried T. N. (2001) N -butyldeoxynojirimycin reduces growth and ganglioside content of experimental mouse brain tumours. *Br. J. Cancer* **84**, 1107–1114.

Sandhoff K. and Kolter T. (2003) Biosynthesis and degradation of mammalian glycosphingolipids. *Philos. Trans. R. Soc. Lond. B Biol. Sci.* **358**, 847–861.

Sango K., Yamanaka S., Hoffmann A. *et al.* (1995) Mouse models of Tay-Sachs and Sandhoff diseases differ in neurologic phenotype and ganglioside metabolism. *Nat. Genet.* **11**, 170–176.

Seyfried T. N., Glaser G. H. and Yu R. K. (1978) Cerebral, cerebellar, and brain stem gangliosides in mice susceptible to audiogenic seizures. *J. Neurochem.* **31**, 21–27.

Seyfried T. N., Bernard D., Mayeda F., Macala L. and Yu R. K. (1984) Genetic analysis of cerebellar lipids in mice susceptible to audiogenic seizures. *Exp. Neurol.* **84**, 590–595.

Sugimoto H., Wakata N., Kishi M., Fujioka T., Kurihara T., Irie Y. and Saito T. (2002) A case of Guillain-Barré syndrome associated with cerebellar ataxia and positive serum anti-GD1b IgG antibody. *J. Neurol.* **249**, 346–347.

Tifft C. J. and Proia R. L. (2000) Stemming the tide: glycosphingolipid synthesis inhibitors as therapy for storage diseases. *Glycobiology* **10**, 1249–1258.

Todorova M. T., Tandon P., Madore R. A., Stafstrom C. E. and Seyfried T. N. (2000) The ketogenic diet inhibits epileptogenesis in EL mice: a genetic model for idiopathic epilepsy. *Epilepsia* **41**, 933–940.

Treiber A., Morand O. and Clozel M. (2007) The pharmacokinetics and tissue distribution of the glucosylceramide synthase inhibitor. *Xenobiotica* **37**, 298–314.

Veech R. L. (2004) The therapeutic implications of ketone bodies: the effects of ketone bodies in pathological conditions: ketosis, ketogenic diet, redox states, insulin resistance, and mitochondrial metabolism. *Prostaglandins Leukot. Essent. Fatty Acids* **70**, 309–319.

Weindruch R. and Walford R. L. (1988) *The retardation of aging and disease by dietary restriction*. Thomas, Springfield, Illinois.

Willenbrock F. W., Neville D. C., Jacob G. S. and Scudder P. (1991) The use of HPLC-pulsed amperometry for the characterization and assay of glycosidases and glycosyltransferases. *Glycobiology* **1**, 223–227.

Williamson D. H., Mellanby J. and Krebs H. A. (1962) Enzymic determination of D(-)-beta-hydroxybutyric acid and acetoacetic acid in blood. *Biochem. J.* **82**, 90–96.

